Supporting Information

Pro-nifuroxazide Self-Assembly Leads to Triggerable Nanomedicine for Anti-Cancer Therapy

Santosh K. Misra,[1,3]†¥ Zhe Wu,[5]† Fatemeh Ostadhossein,[1,3] Mao Ye, [1,3] Kingsley Boateng,[8] Klaus Schulten,[2,5] Emad Tajkhorshid,[2,6] and Dipanjan Pan[1,2,3,4,7*]

[1]Department of Bioengineering, University of Illinois at Urbana-Champaign, USA, 61801

[2]Beckman Institute of Advanced Science and Technology, University of Illinois at Urbana-Champaign, Illinois, USA, 61801

[3]Mills Breast Cancer Institute, Carle Foundation Hospital, 502 N. Busey, Urbana, Illinois, USA, 61801

[4]Department of Materials Science and Engineering, University of Illinois-Urbana Champaign, Illinois, USA, 61801

[5]Center for the Physics of Living Cells, Department of Physics, University of Illinois-Urbana Champaign, Illinois, USA, 61801

[6]Department of Biochemistry, University of Illinois-Urbana Champaign, Illinois, USA, 61801

[7]Department of Materials Science and Engineering, University of Illinois-Urbana Champaign, Illinois, USA, 61801

[8]Carl R. Woese Institute for Genomic Biology, University of Illinois-Urbana Champaign, Illinois, USA, 61801

†Authors contributed equally to this work.

*Corresponding Author: dipanjan@illinois.edu

Content **Page**

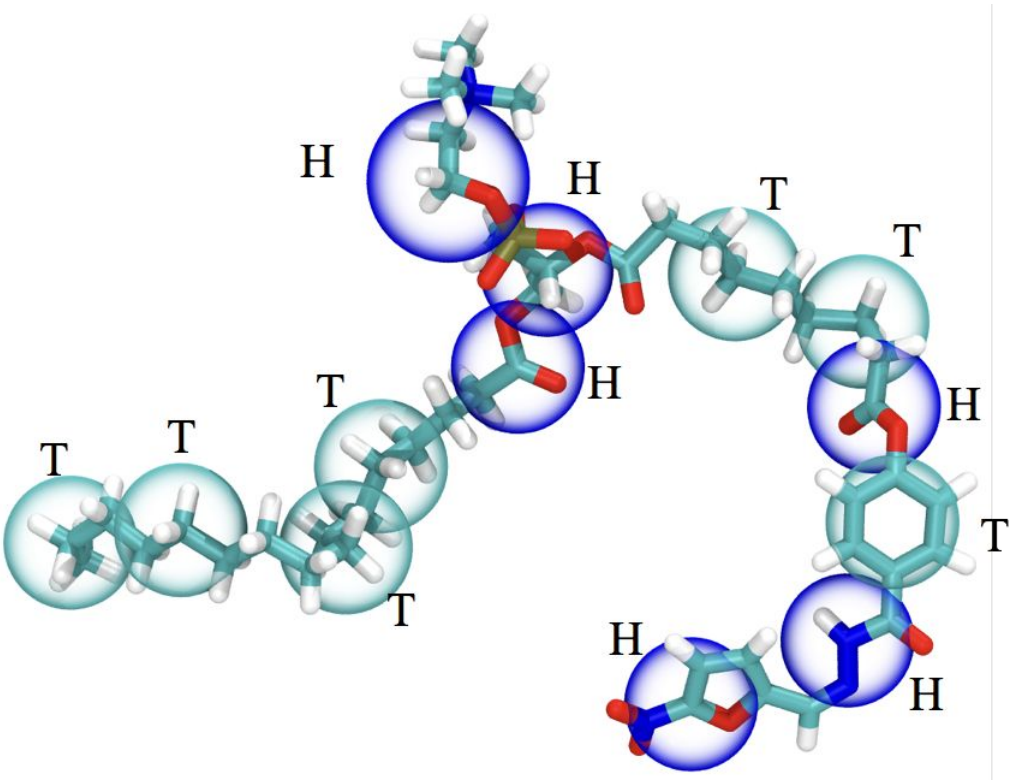

Figure S1. Mapping from atomistic structure to a coarse-grained DPD model of pro-nifuroxazide. Coarse-grained particle types are labeled by letters.

Table S1. Coarse-grained model parameters for pro-nifuroxazide and polyethylene glycol cetyl ether

Non-bond interaction force parameter a_{ij} (unit: k_BT/r_0)

	H	**T**	**W**
H	25	50	35
T	50	25	75
W	35	75	25

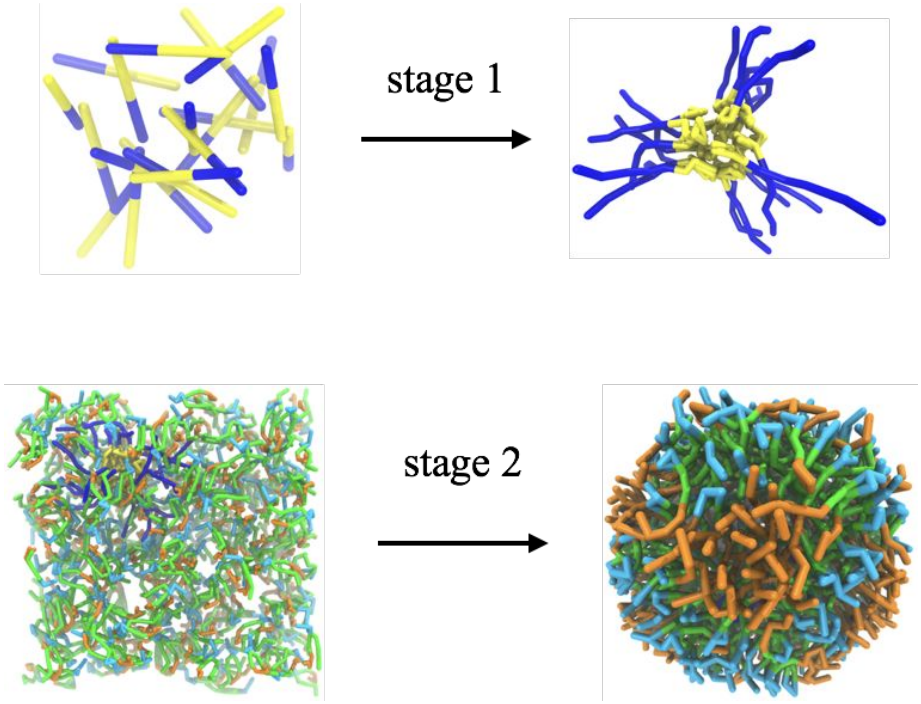

Figure S2. Two stages of self-assembly DPD simulations: (1) formation of a core particle with PEGCE, and, (2) formation of prodrug nanoparticle.

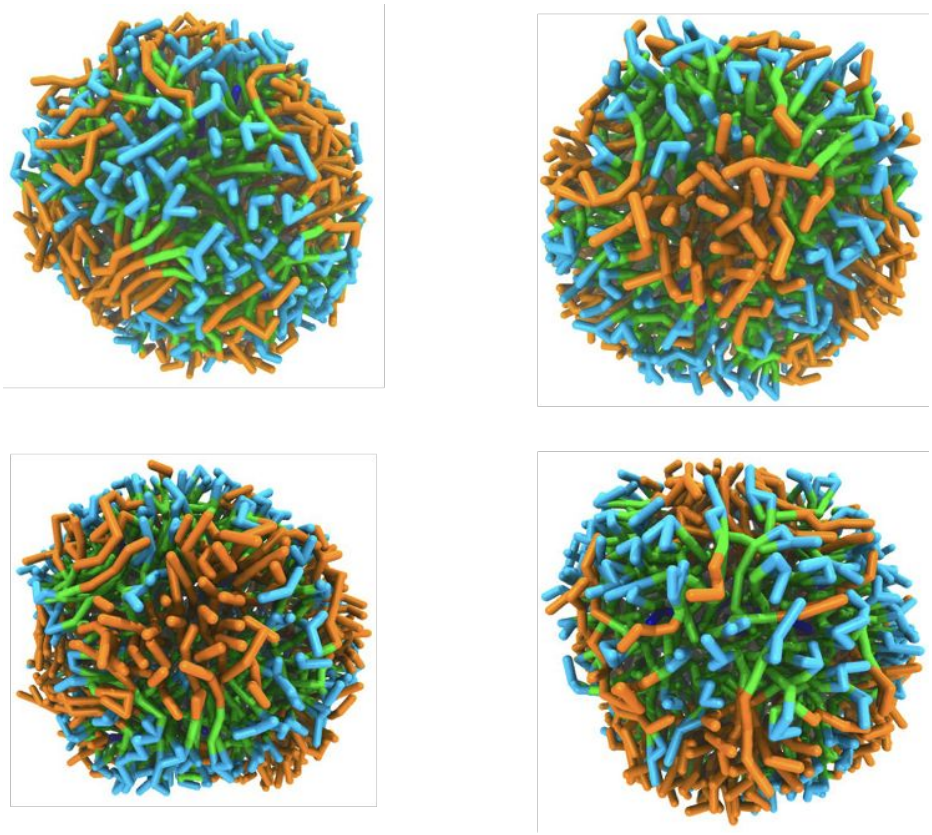

Figure S3. Examples of prodrug nanoparticle structures resulted from independent DPD simulations.

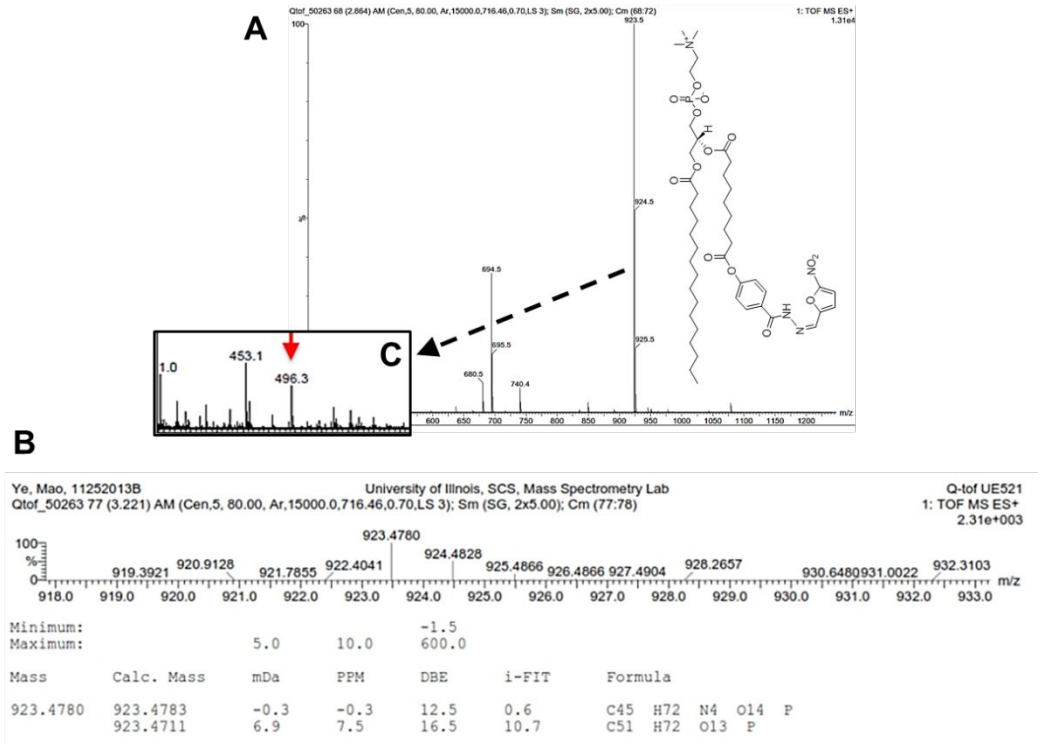

Figure S4. Chemical characterization of pro-nifuroxazide synthesized from nifuroxazide small molecule. LRMS (A) and HRMS (B) analyses after incubation with phosphate buffer at pH 4.5 and after treatment with phospholipase 2 (PLA2) m/z: 496.34 (MH+ for nifuroxazide calculated for $C_{24}H_{51}NO_7P$), calculated 496.64 MH+ for liberated lysoPC (C).

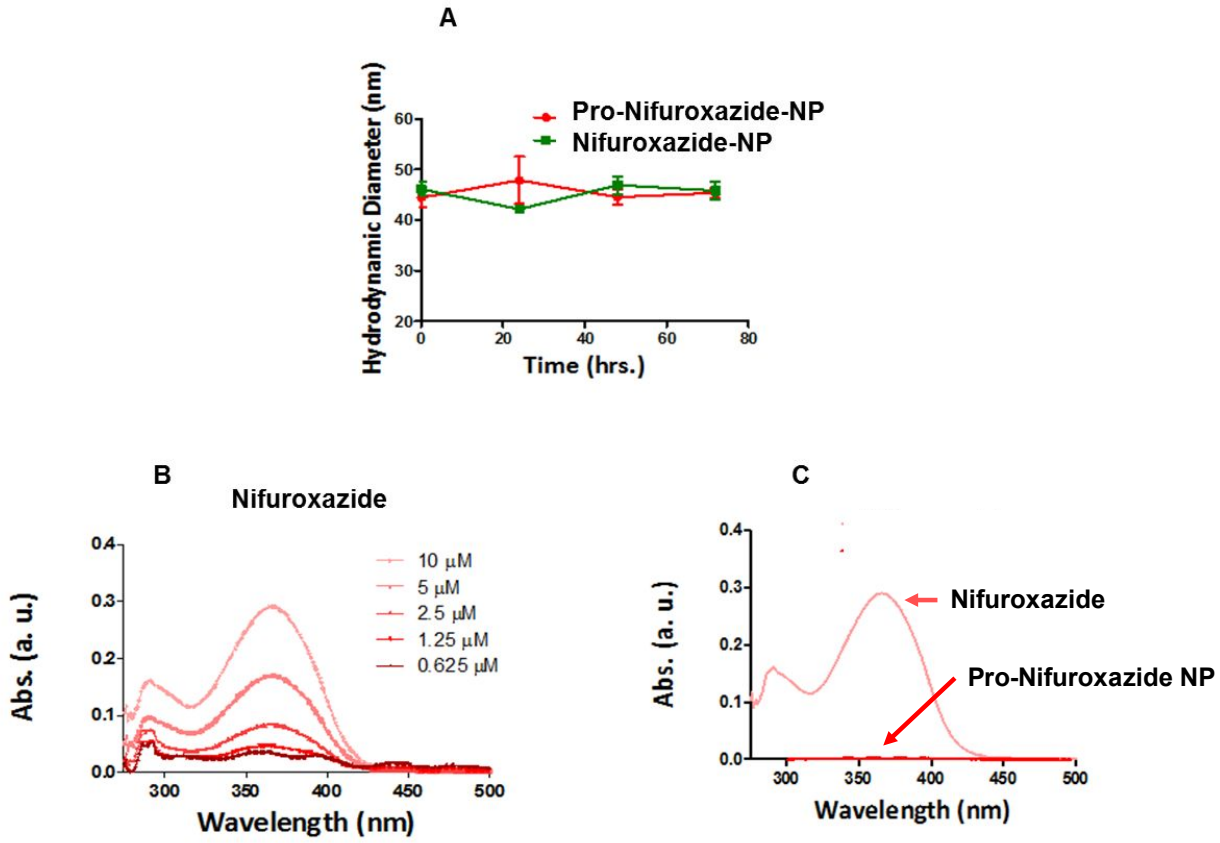

Figure S5. Characterizations of drug and nano-prodrug. (A) stability of nano-prodrug; (B) UV-vis spectroscopic pattern varied with change in different concentration of nifuroxazide (10 to 0.625 µM) and (C) decrease in absorbance of nifuroxazide with formation of Pro-nifuroxazide NP.

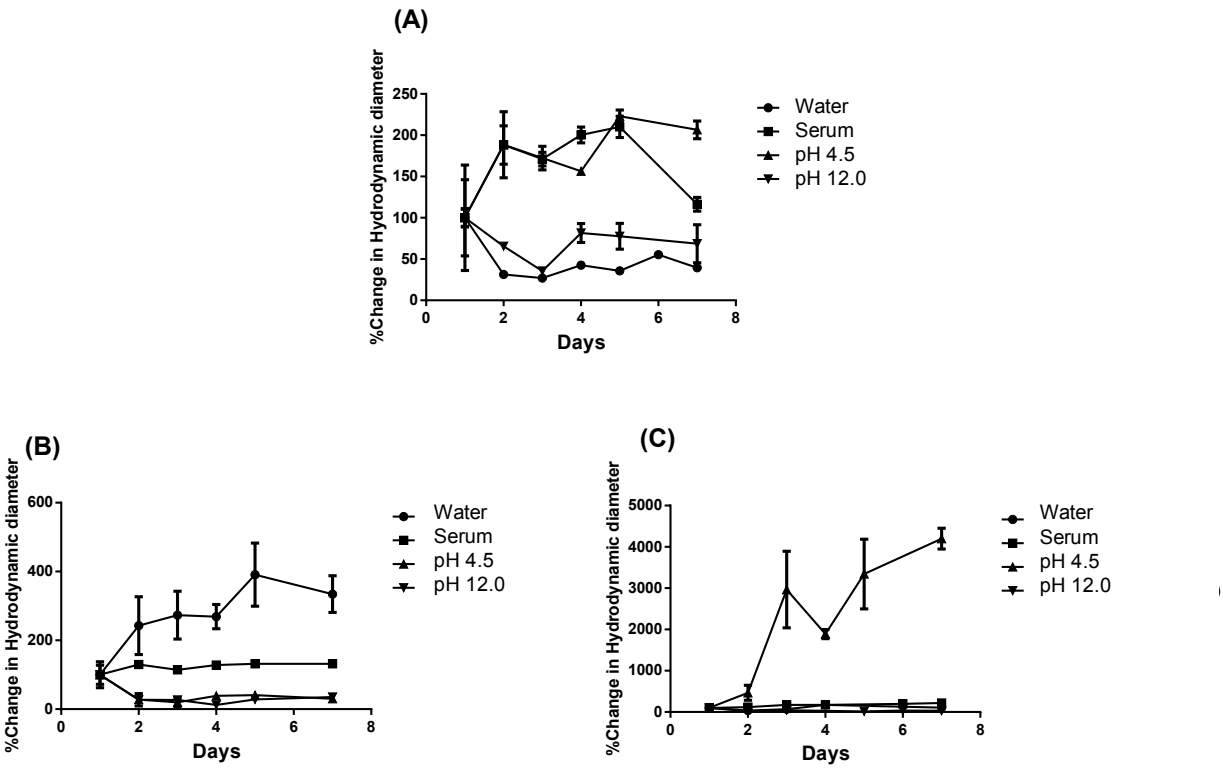

Figure S6. Stability of different formulations in various mediums. Hydrodynamic diameter of formulations (A) Lipid-NPs, (B) Pro-Nifuroxazide NP (no-core) and (C) Pro-nifuroxazide NP were acquired at 1, 2, 3, 4, 5, 6 and 7 days after incubation with water, Serum, pH 4.5 and pH 12.0 at 37 °C.

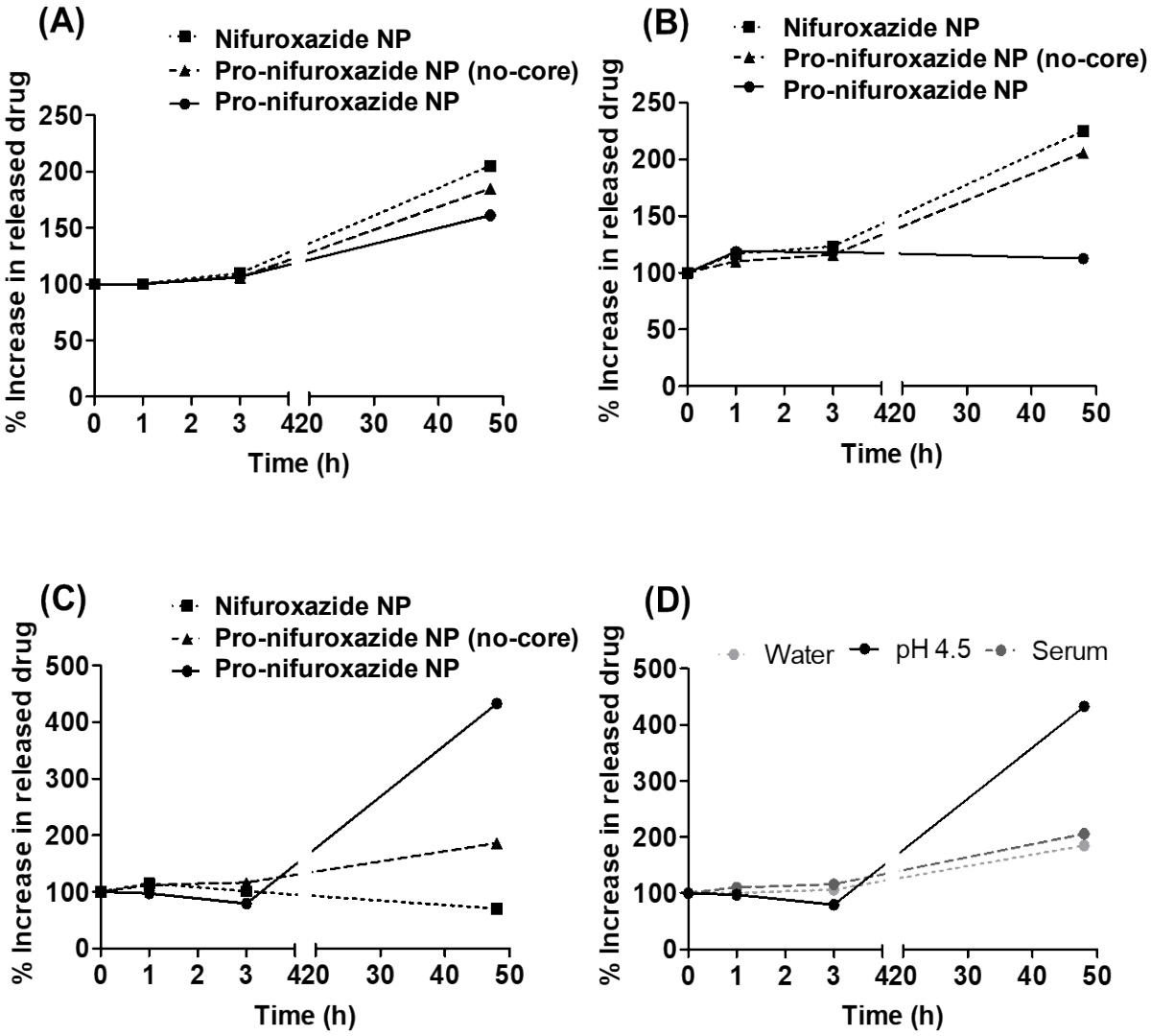

Figure S7. Release kinetics of nifuroxazide from different nanoparticles incubated with different suspension mediums including (A) water; (B) blood serum (10%) and (C) pH 4.5. (D) Comparison of nifuroxazide release from Pro-nifuroxazide NPs in different mediums after 48h of incubation. Suspensions were incubated at 37 °C for 1, 3 and 48h.

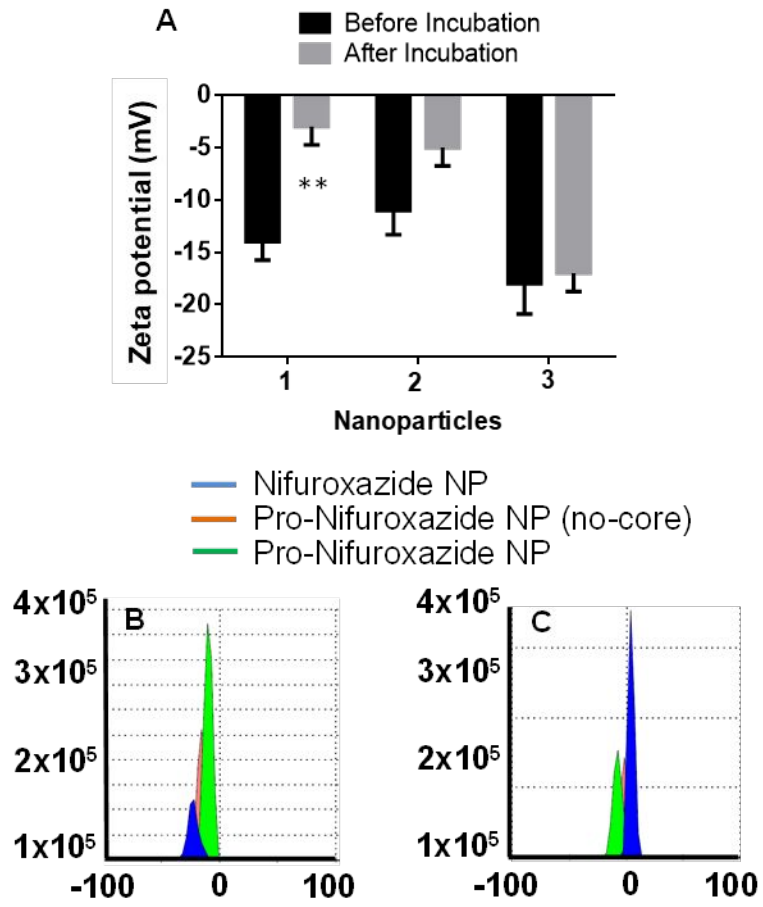
A
Before Incubation
After Incubation
Zeta potential (mV)
0
-5
-10
-15
-20
-25
**
1
2
3
Nanoparticles
Nifuroxazide NP
Pro-Nifuroxazide NP (no-core)
Pro-Nifuroxazide NP
4x10^5
3x10^5
2x10^5
1x10^5
B
-100
0
100
4x10^5
3x10^5
2x10^5
1x10^5
C
-100
0
100

Figure S8. (A) Protein interaction properties of different nanoparticles presented as (1) Nifuroxazide NP, Pro-Nifuroxazide NP (no-core) and (3) Pro-Nifuroxazide NPs. Formulations were incubated with 10% FBS for 4h at 37 °C before performing the zeta potential experiments. Changes in electrophoretic potential after incubation indicate formation of protein corona. Statistical analysis was performed using ONE Way ANOVA with post Bonferroni test. Here ** represents p values < 0.01. Zeta potential of Nifuroxazide NP (blue), Pro-Nifuroxazide NP (no-core) (orange) and Pro-Nifuroxazide NPs (green) (B) before and (C) after 7 days of incubation with 10% FBS.

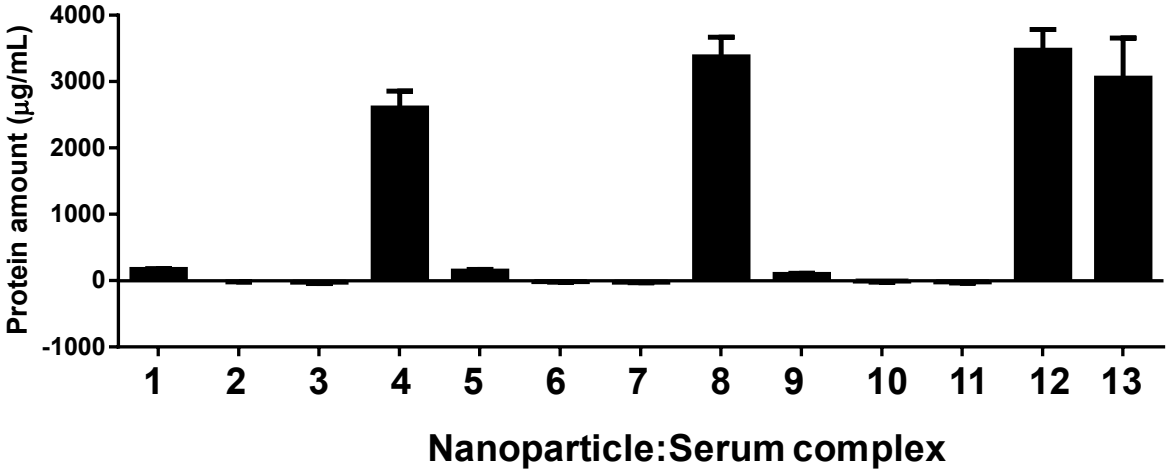

Figure S9. Protein interaction efficiency of Nifuroxazide NP, Pro-Nifuroxazide NP (no-core) and Pro-Nifuroxazide NPs after 4h incubation at 37 °C. A Bradford's assay was performed on nanoparticles coated with protein and remaining protein unbound. Here nanoparticle:serum complexes are represented as **1**: Nifuroxazide NP coated with 25% serum protein; **2**: Nifuroxazide NP coated with 5% serum protein; **3**: Nifuroxazide NP coated with 1% serum protein; **4**: Total amount of serum protein added to Nifuroxazide NPs; **5**: Pro-Nifuroxazide NP (no-core) coated with 25% serum protein; **6**: Pro-Nifuroxazide NP (no-core) coated with 5% serum protein; **7**: Pro-Nifuroxazide NP (no-core) coated with 1% serum protein; **8**: Total amount of serum protein added to Pro-Nifuroxazide NPs (no-core); **9**: Pro-Nifuroxazide NP coated with 25% serum protein; **10**: Pro-Nifuroxazide NP coated with 5% serum protein; 11: Pro-Nifuroxazide NP coated with 1% serum protein; **12**: Total amount of serum protein added to Pro-Nifuroxazide NPs and **13**: Total amount of protein in used volume of FBS.

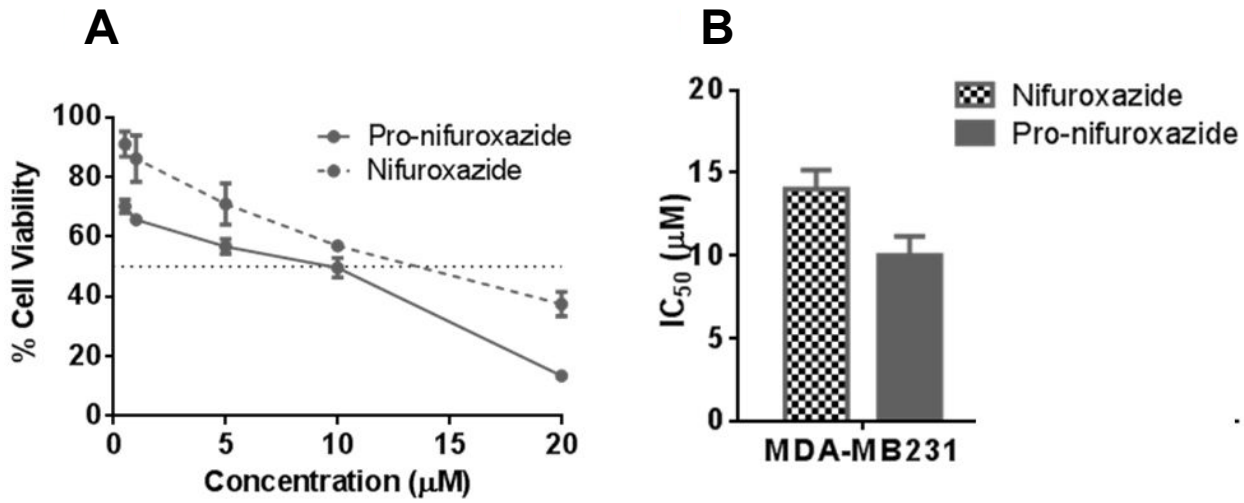

Figure S10. *In vitro* analysis of cancer cell growth regression after treatment with nifuroxazide and pro-nifuroxazide. (A) MTT assay performed on MDA-MB231 cells after 72h treatment of nifuroxazide and pro-nifuroxazide at concentration ranging from 0.5 to 20 μM and (B) IC_{50} values of nifuroxazide and prodrug in MDA-MB231 cells.

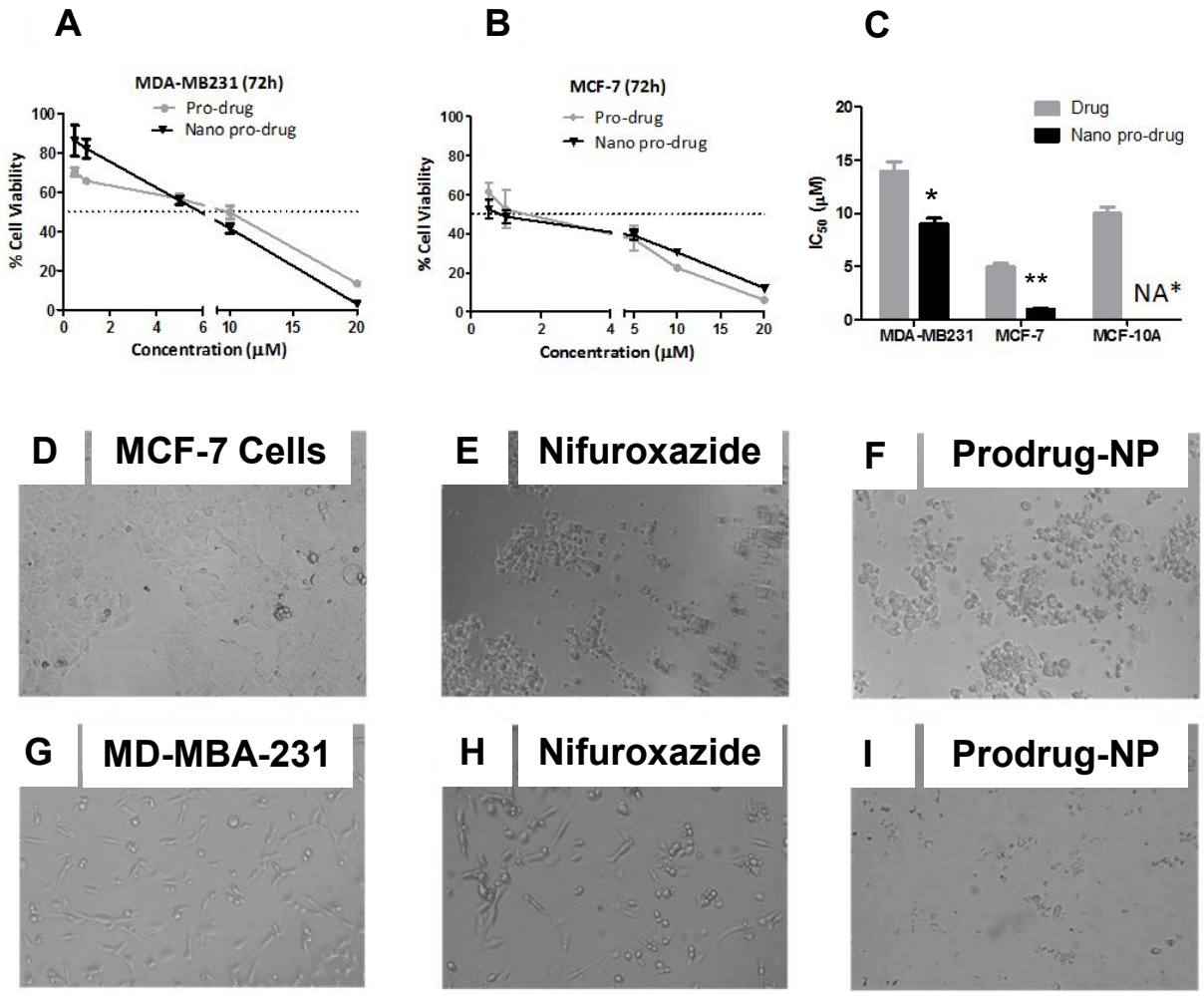

Figure S11. *In vitro* analysis of cancer cell growth regression after treatment with nifuroxazide and nano-prodrug. MTT assay performed on (A) MDA-MB231 and (B) MCF-7 cells after 72h treatment of nifuroxazide and pro-nifuroxazide-NP at concentration ranging from 0.5 to 20 µM and (C) IC_{50} summarized for all the cell lines. Bright field images of MCF-7 cells (D) untreated and treated with (E) nifuroxazide; (F) pro-nifuroxazide and MDA-MB231 cells (G) untreated and treated with (H) nifuroxazide; (I) pro-nifuroxazide-NP treated at concentration of 20 µM. Biostatistical analysis was performed using ONE Way ANOVA with post Bonferroni test. Here * and ** represent p values <0.05 and 0.01, respectively.

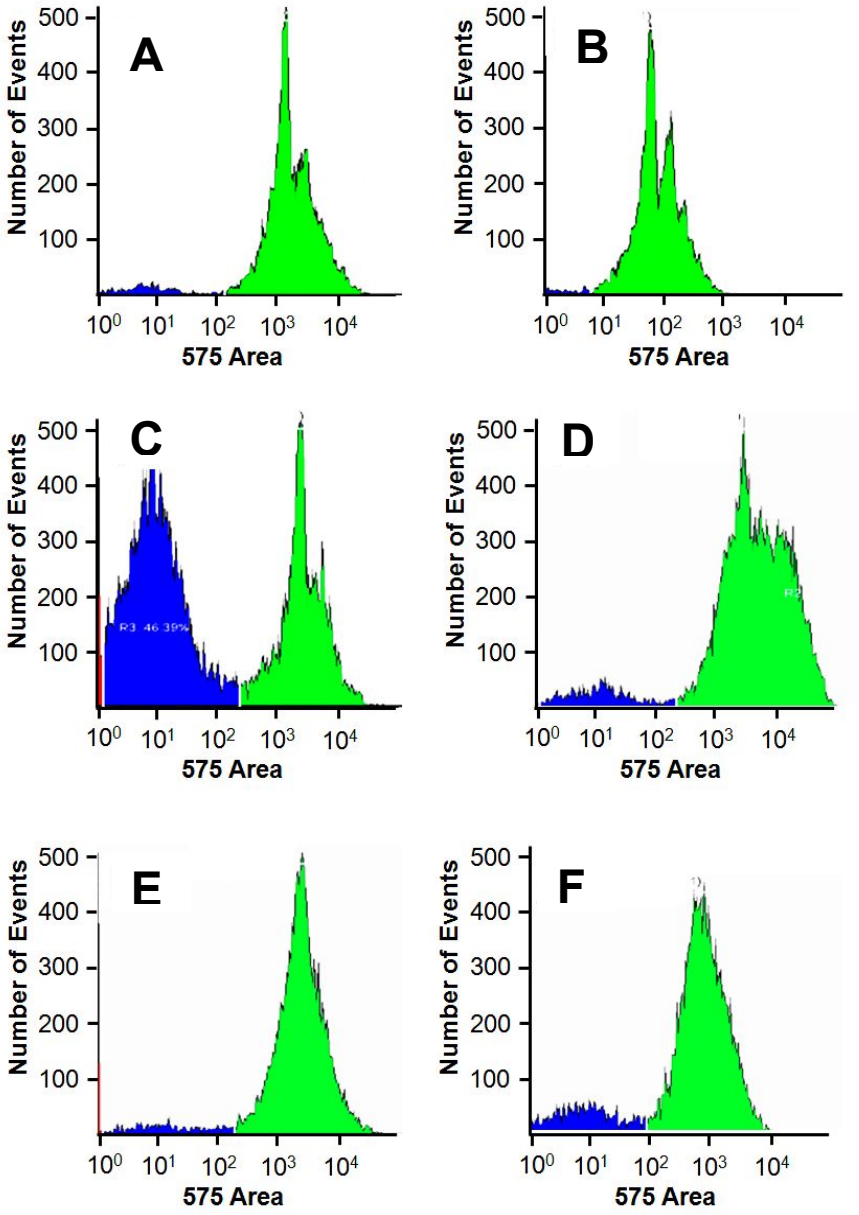

Figure S12. Representative histogram of PI stained MCF-7 cells treated with (A) untreated and treated with (B) nifuroxazide and (C) pro-nifuroxazide-NP (nano-prodrug) and MDA-MB231 (D) untreated and treated with (E) nifuroxazide and (F) pro-nifuroxazide-NP (nano-prodrug).

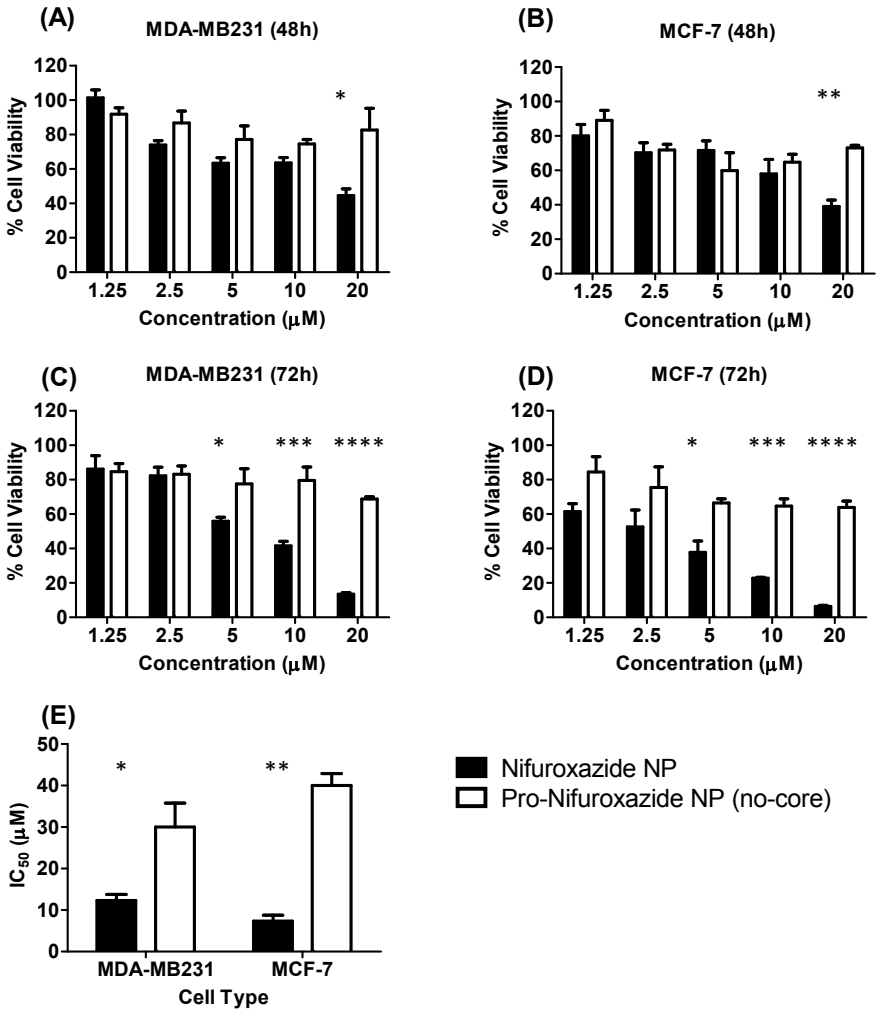

Figure S13. MTT assay performed on MCF-7 and MDA-MB231 using cored nanoparticles with loaded nifuroxazide (Nifuroxazide NP) and non-cored nanoparticles with Pro-nifuroxazide (Pro-nifuroxazide NP (no-core)). Experiments were performed in MDA-MB231 cells at (A) 48 and (C) 72h time points, MCF-7 cells at (B) 48 and (D) 72h time point and comparison for IC50 values in MCF-7 and MDA-MB231 cells. Experiments were performed for two different time points and nifuroxazide concentration of 1.25, 2.5, 5, 10 and 20 μM. Biostatistical analysis was performed using ONE Way ANOVA with post Bonferroni test. Here *, **, *** and **** represent p values <0.05, 0.01, 0.001 and 0.0001, respectively.

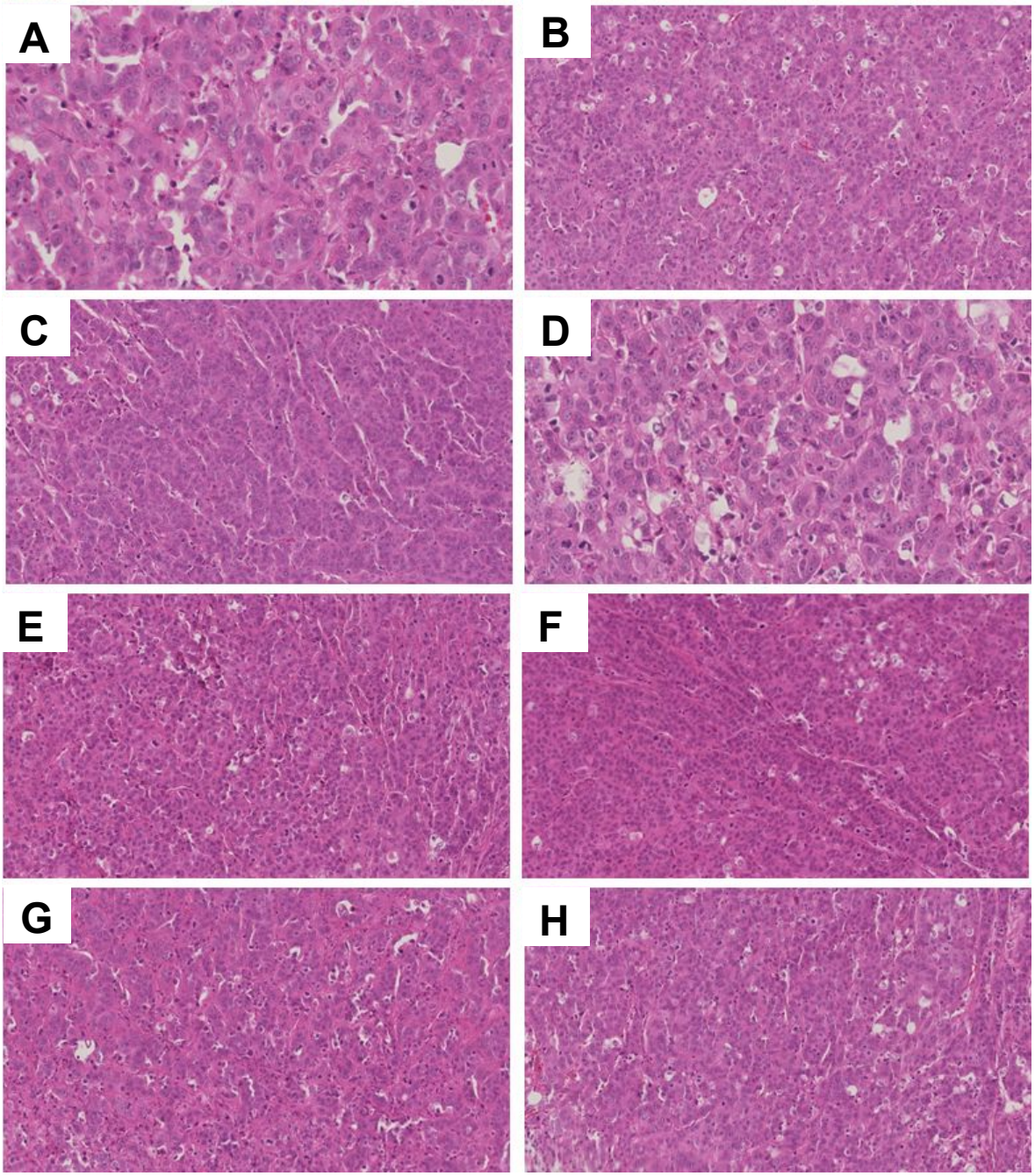

Figure S14. Representative H & E sections of tumors treated with buffer (A-H). Here sections are from same tumors on same or different animals including (A-D) from animal #2 and (E-H) from Animal #9 as each represent individual tumor. Sections were stained with histamine (red) and eosin (blue).

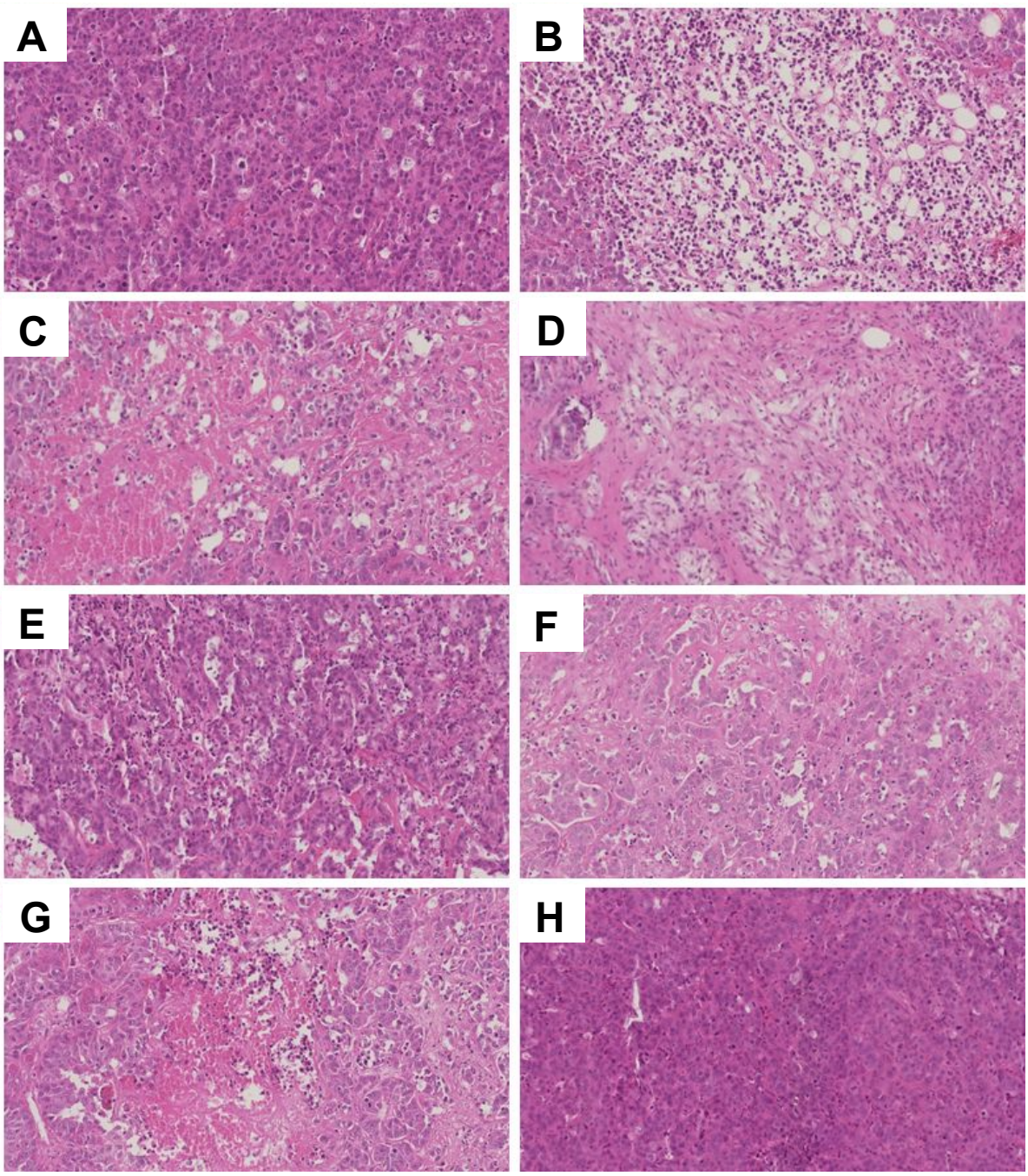

Figure S15. Representative H&E sections of tumors treated with nano-prodrug (A-H). Here sections are from same tumors on same or different animals including (A-D) from animal #1 and (E-H) from Animal #17 as each represent individual tumor. Sections were stained with histamine (red) and eosin (blue).

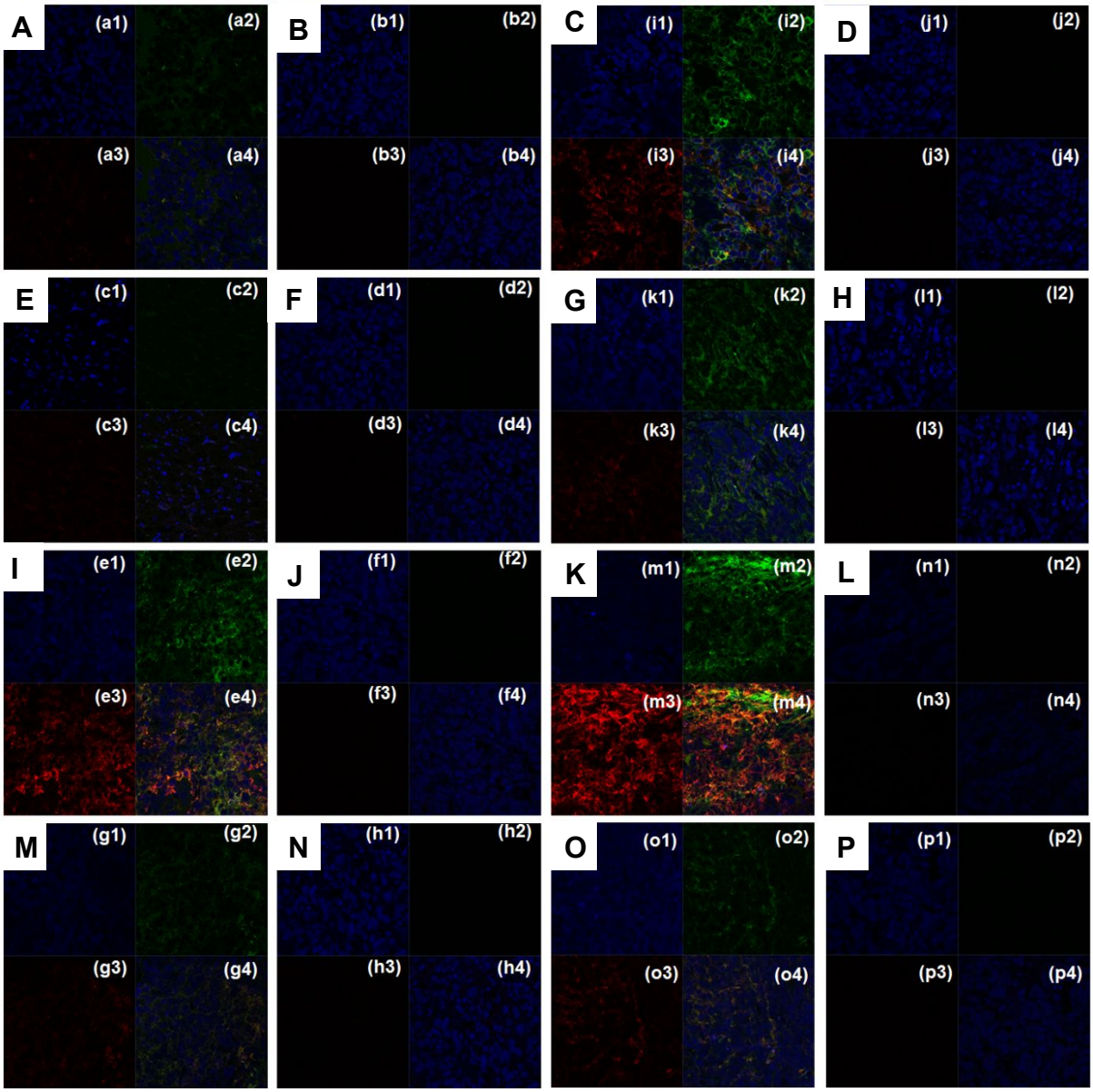

Figure S16. Representative immune-labelled cross sections of tumors treated with buffer (A-P). Here sections are from same tumors on same or different animals including (A and B); (C and D); (E and F); (G and H) from animal #1 and (I and J); (K and L); (M and N) and (O and P) from Animal #17. Sections were treated with or without pSTAT-3 antibody (red) against antibody treated against common unaffected protein β-actin (green). All the sections from tumors were also stained with DAPI (blue) to visualize cell nuclei. A low level of pSTAT-3 in tumors treated with pro- nifuroxazide NP were visualized across all the section.

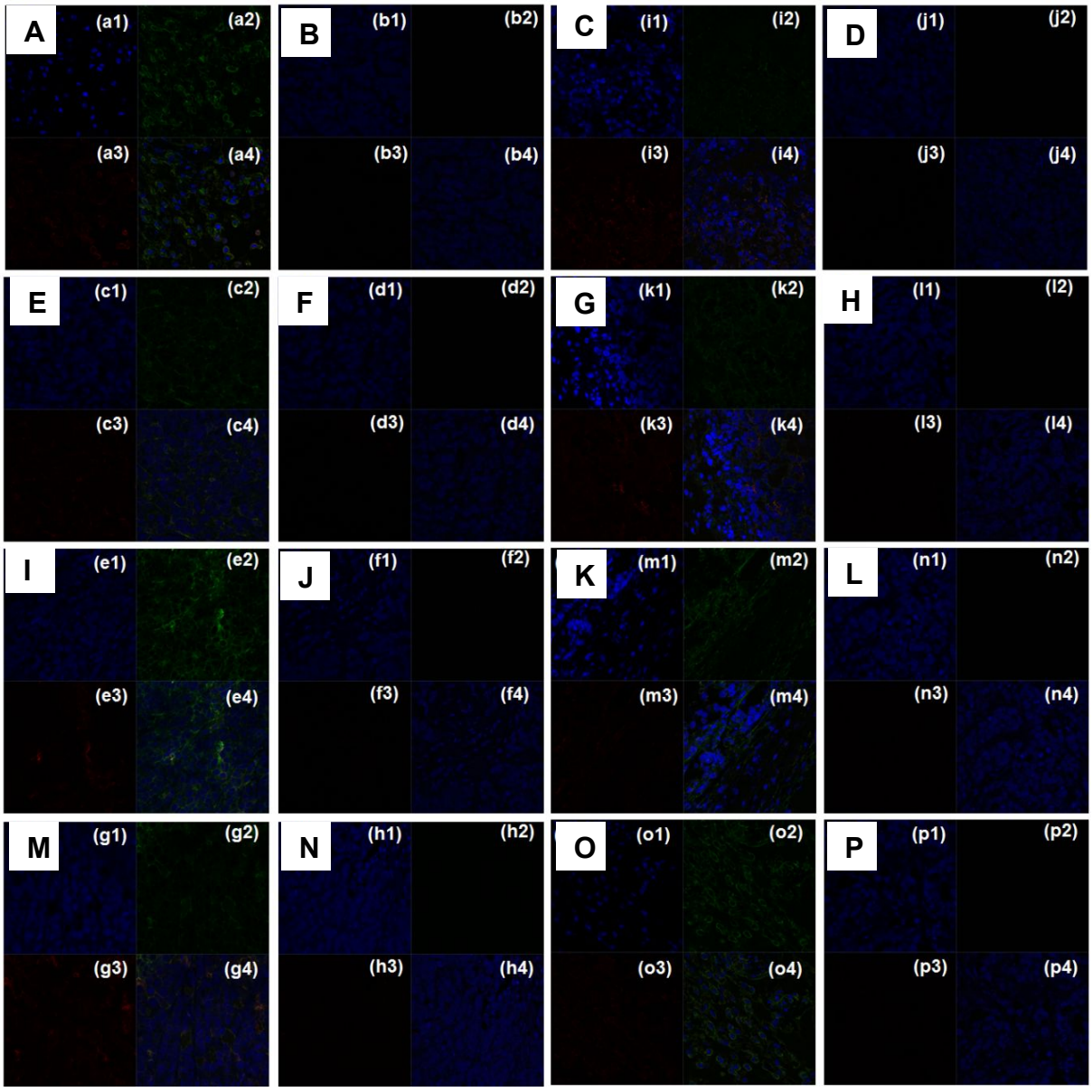

Figure S17. Representative immune-labelled cross sections of tumors treated with nano-prodrug (A-P). Here sections are from same tumors on same or different animals including (A and B); (C and D); (E and F); (G and H) from animal #1 and (I and J); (K and L); (M and N) and (O and P) from Animal #17. Sections were treated with or without pSTAT-3 antibody (red) against antibody treated against common unaffected protein β-actin (green). All the sections from tumors

were also stained with DAPI (blue) to visualize cell nuclei. A low level of pSTAT-3 in tumors treated with pro-nifuroxazide NP were visualized across all the sections.

Atomistic CGenFF parameters for pro-nifuroxazide

Parameter file:

```
* Parameters generated by analogy by
* CHARMM General Force Field (CGenFF) program version 0.9.7.1 beta
*
BONDS
CG2DC1 CG2R51  365.00     1.4500 !
CG2R51 NG2O1   230.00     1.4020 !
CG2R61 OG302   230.00     1.3820 !

ANGLES
CG2R51 CG2DC1 NG2D1    56.00    117.00 !
CG2R51 CG2DC1 HGA4     32.00    120.00 !
CG2DC1 CG2R51 CG2R51   45.80    130.00 !
CG2DC1 CG2R51 OG2R50   45.80    124.00 !
CG2R51 CG2R51 NG2O1    55.00    125.50 !
NG2O1  CG2R51 OG2R50   65.00    127.80 !
CG2R61 CG2R61 OG302   110.00    120.00 !
CG2R51 NG2O1  OG2N1    65.00    116.00 !
CG2O2  OG302  CG2R61  185.00    120.00 !

DIHEDRALS
NG2D1  CG2DC1 CG2R51 CG2R51     1.6000  2   180.00 !
NG2D1  CG2DC1 CG2R51 OG2R50     1.6000  2   180.00 !
HGA4   CG2DC1 CG2R51 CG2R51     0.6000  2   180.00 !
HGA4   CG2DC1 CG2R51 OG2R50     0.6000  2   180.00 !
CG2R51 CG2DC1 NG2D1  NG2S1     12.0000  2   180.00 !
```

```
CG321  CG2O2  OG302  CG2R61     2.0500  2   180.00 !
OG2D1  CG2O2  OG302  CG2R61     0.9650  1   180.00 !
OG2D1  CG2O2  OG302  CG2R61     3.8500  2   180.00 !
CG2DC1 CG2R51 CG2R51 CG2R51    15.0000  2   180.00 !
CG2DC1 CG2R51 CG2R51 HGR51      1.0000  2   180.00 !
CG2R51 CG2R51 CG2R51 NG2O1      8.5000  2   180.00 !
NG2O1  CG2R51 CG2R51 HGR51      2.7000  2   180.00 !
CG2R51 CG2R51 NG2O1  OG2N1      0.9000  2   180.00 !
OG2R50 CG2R51 NG2O1  OG2N1      0.9000  2   180.00 !
CG2DC1 CG2R51 OG2R50 CG2R51     7.5000  2   180.00 !
NG2O1  CG2R51 OG2R50 CG2R51     8.5000  2   180.00 !
CG2R61 CG2R61 CG2R61 OG302      3.1000  2   180.00 !
OG302  CG2R61 CG2R61 HGR61      2.4000  2   180.00 !
CG2R61 CG2R61 OG302  CG2O2      1.2000  2   180.00 !

IMPROPERS
CG2DC1 CG2R51 NG2D1  HGA4      30.0000  0     0.00 !

END
```

Parameter file for linkage between nifuroxazide moiety and PAzPC:

```
BONDS
CG321  CTL2  222.500     1.530   ! alkanes, 3/92

ANGLES
CG321  CG321  CTL2  58.350    113.60   11.16   2.561  ! alkane, 3/92
HGA2   CG321  CTL2  26.500    110.10   22.53   2.179  ! alkane, 4/98
CG321  CTL2   CTL2  58.350    113.60   11.16   2.561  ! alkane, 3/92
CG321  CTL2   HAL2  26.500    110.10   22.53   2.179  ! alkane, 4/98

DIHEDRALS
CG2O2  CG321  CG321  CTL2      0.000   5   180.00 ! propyl ester, 6/07
CG2O2  CG321  CG321  CTL2      0.317   3   180.00 ! propyl ester, 6/07
CG2O2  CG321  CG321  CTL2      0.557   2     0.00 ! propyl ester, 6/07
CG2O2  CG321  CG321  CTL2      0.753   1     0.00 ! propyl ester, 6/07
X    CG321 CG321 X       0.1900  3     0.00 ! alkane, 4/98, yin and mackerell
X    CG321 CTL2  X       0.1900  3     0.00 ! alkane, 4/98, yin and mackerell
CG321  CG321  CTL2   CTL2     0.101   2     0.00 ! alkane, 7/08, jbk
CG321  CG321  CTL2   CTL2     0.142   3   180.00 ! alkane, 7/08, jbk
CG321  CG321  CTL2   CTL2     0.074   4     0.00 ! alkane, 7/08, jbk
CG321  CG321  CTL2   CTL2     0.097   5     0.00 ! alkane, 7/08, jbk

IMPROPER
OG2D1  X    X    CG2O2        100.00    0     0.00 ! acetic acid
OG2D1  X    X    CG2O1        120.0000  0     0.0000 ! ALLOW   PEP POL ARO

NONBONDED nbxmod  5 atom cdiel shift vatom vdistance vswitch -
cutnb 14.0 ctofnb 12.0 ctonnb 10.0 eps 1.0 e14fac 1.0 wmin 1.5

END
```

Topology file for nifuroxazide moiety, which includes atom type, charge, bonding information:

```
* Toppar stream file generated by
* CHARMM General Force Field (CGenFF) program version 0.9.7.1 beta
* For use with CGenFF version 2b8
*
read rtf card append
* Topologies generated by
* CHARMM General Force Field (CGenFF) program version 0.9.7.1 beta
*
36 1

RESI NIF       0.000 !
GROUP           ! CHARGE
ATOM C1     CG2R61 -0.101 !
ATOM H3     HGR61   0.115 !
ATOM C2     CG2R61  0.216 !
ATOM O1     OG302  -0.454 !
ATOM C4     CG2R61 -0.101 !
ATOM H4     HGR61   0.115 !
ATOM C5     CG2R61 -0.063 !
ATOM H5     HGR61   0.115 !
ATOM C6     CG2R61 -0.071 !
ATOM C7     CG2R61 -0.063 !
ATOM H6     HGR61   0.115 !
ATOM C8     CG2O2   0.927 !
ATOM C9     CG321  -0.221 !
ATOM H1     HGA2    0.090 !
ATOM H2     HGA2    0.090 !
ATOM C3     CG321  -0.181 !
ATOM C31    CG331  -0.273 !
ATOM H311   HGA3    0.090 !
ATOM H312   HGA3    0.090 !
ATOM H313   HGA3    0.090 !
ATOM H32    HGA2    0.090 !
```

```
ATOM H33    HGA2    0.090 !
ATOM O2     OG2D1  -0.644 !
ATOM C10    CG2O1   0.458 !
ATOM N2     NG2S1  -0.344 !
ATOM N1     NG2D1  -0.315 !
ATOM H9     HGP1    0.305 !
ATOM O3     OG2D1  -0.406 !
ATOM C11    CG2DC1 -0.279 !
ATOM H10    HGA4    0.239 !
ATOM C12    CG2R51 -0.273 !
ATOM H7     HGR51   0.196 !
ATOM C13    CG2R51 -0.273 !
ATOM H8     HGR51   0.196 !
ATOM C14    CG2R51  0.508 !
ATOM O4     OG2R50 -0.342 !
ATOM C15    CG2R51  0.511 !
ATOM N3     NG2O1   0.408 !
ATOM O5     OG2N1  -0.325 !
ATOM O6     OG2N1  -0.325 !

BOND C1   H3
BOND C1   C2
BOND C1   C7
BOND C2   O1
BOND C2   C4
BOND O1   C8
BOND C4   H4
BOND C4   C5
BOND C5   H5
BOND C5   C6
BOND C6   C7
BOND C6   C10
BOND C7   H6
```

```
BOND C8   C9
BOND C8   O2
BOND C9   H1
BOND C9   H2
BOND C9   C3
BOND C3   C31
BOND C3   H32
BOND C3   H33
BOND C31  H311
BOND C31  H312
BOND C31  H313
BOND C10  N2
BOND C10  O3
BOND N2   N1
BOND N2   H9
BOND N1   C11
BOND C11  H10
BOND C11  C14
BOND C12  H7
BOND C12  C13
BOND C12  C15
BOND C13  H8
BOND C13  C14
BOND C14  O4
BOND O4   C15
BOND C15  N3
BOND N3   O5
BOND N3   O6
IMPR C8    C9    O2    O1
IMPR C10   C6    N2    O3
IMPR C11   C14   N1    H10

END
```

References:

(1) Shillcock, J. C.; Lipowsky, R. Equilibrium Structure and lateral stress distribution of amphiphilic bilayers from dissipative particle dynamics simulations. *J. Chem. Phys.* 2002, 117, 5048.

(2) Groot, R. D.; Rabone, K. L. Mesoscopic Simulation of Cell Membrane Damage, Morphology Change and Rupture by Nonionic Surfactants. *Biophys. J.* **2001,** 81, 725.

(3) Yamamoto, S.; Maruyama, Y.; Hyodo, S. Coarse Gaining and Scaling in Dissipative Particle Dynamics. *J. Chem. Phys.* **2002**, 116, 5842.

(4) Ortiz, V.; Nielsen, S. O.; Discher, D. E.; Klein, M. L.; Lipowsky, R.; Shillcock, J. Dissipative particle dynamics simulations of polymersomes. *J. Phys. Chem. B* **2005**, 109, 17708.

(5) Kranenburg, M.; Nicolas, J.; Smit, B. Comparison of Mesoscopic Phospholipid–water Models. *Phys. Chem. Chem. Phys.* **2004**, 6, 4142.

(6) Plimpton, S. Fast Parallel Algorithms for Short-Range Molecular Dynamics. *J. Comp. Phys.* **1995**, 117, 1.

(7) Phillips, J. C.; Braun, R.; Wang, W.; Gumbart, J.; Tajkhorshid, E.; Villa, E.; Chipot, C.; Skeel, R. D.; Kalé, L.; Schulten, K. Scalable Molecular Dynamics with NAMD. *J. Comput. Chem.* 2005, 26, 1781.

(8) Vanommeslaeghe, K.; Hatcher, E.; Acharya, C.; Kundu, S.; Zhong, S.; Shim, J.; Darian, E.; Guvench, O.; Lopes, P.; Vorobyov, I.; Mackerell; AD Jr. CHARMM General Force Field: A Force Field for Drug-Like Molecules Compatible with the CHARMM All-Atom Additive Biological Force Fields. *J. Comput. Chem.* **2010**, 31, 671–690.

(9) Klauda, J. B.; Venable, R. M.; Freites, J. A.; O'Connor, J. W.; Tobias, D. J.; Mondragon-Ramirez, C.; Vorobyov, I.; MacKerell, A. D., Jr.; Pastor, R. W. Update of the CHARMM All-Atom Additive Force Field for Lipids: Validation on Six Lipid Types. *J. Phys. Chem. B* **2010**, 114, 7830–7843.

(10) MacKerell, A. D., Jr.; Bashford, D.; Bellott, M.; Dunbrack, R. L., Jr.; Evanseck, J. D.; Field, M. J.; Fischer, S.; Gao, J.; Guo, H.; Ha, S.; Joseph-McCarthy, D.; Kuchnir, L., Kuczera, K.; Lau, F. T. K.; Mattos, C.; Michnick, S.; Ngo, T.; Nguyen, D. T.; Prodhom, B.; Reiher, W. E.; Roux, B.;

Schlenkrich, M.; Smith, J. C.; Stote, R.; Straub, J.; Watanabe, M.; Wiórkiewicz-Kuczera, J.; Yin, D.; Karplus, M. All-Atom Empirical Potential for Molecular Modeling and Dynamics Studies of Proteins. *J. Phys. Chem. B* **1998**, 102, 3586–3616.

(11) Darden, T.; York, D.; Pedersen, L. G. Particle Mesh Ewald: An N3log(N) Method for Ewald Sums in Large systems. *J. Chem. Phys.* **1993**, 98, 10089–10092.

(12) Tuckerman, M.; Berne, B. J.; Martyna, G. J. Reversible Multiple Time Scale Molecular Dynamics. *J. Chem. Phys.* **1992**, 97, 1990–2001.

(13) Miyamoto, S.; Kollman, P. A. Settle: An Analytical Version of the SHAKE and RATTLE Algorithm for Rigid Water Models. *J. Comput. Chem.* **1992**, 13, 952–962.

(14) Andersen, H. C. Rattle: A "Velocity" Version of the Shake Algorithm for Molecular Dynamics Calculations. *J. Comput. Phys.* **1983**, 52, 24–34.

(15) Grossfield, A. WHAM: The Weighted Histogram Analysis Method, version 2.0.9, http://membrane.urmc.rochester.edu/content/wham.